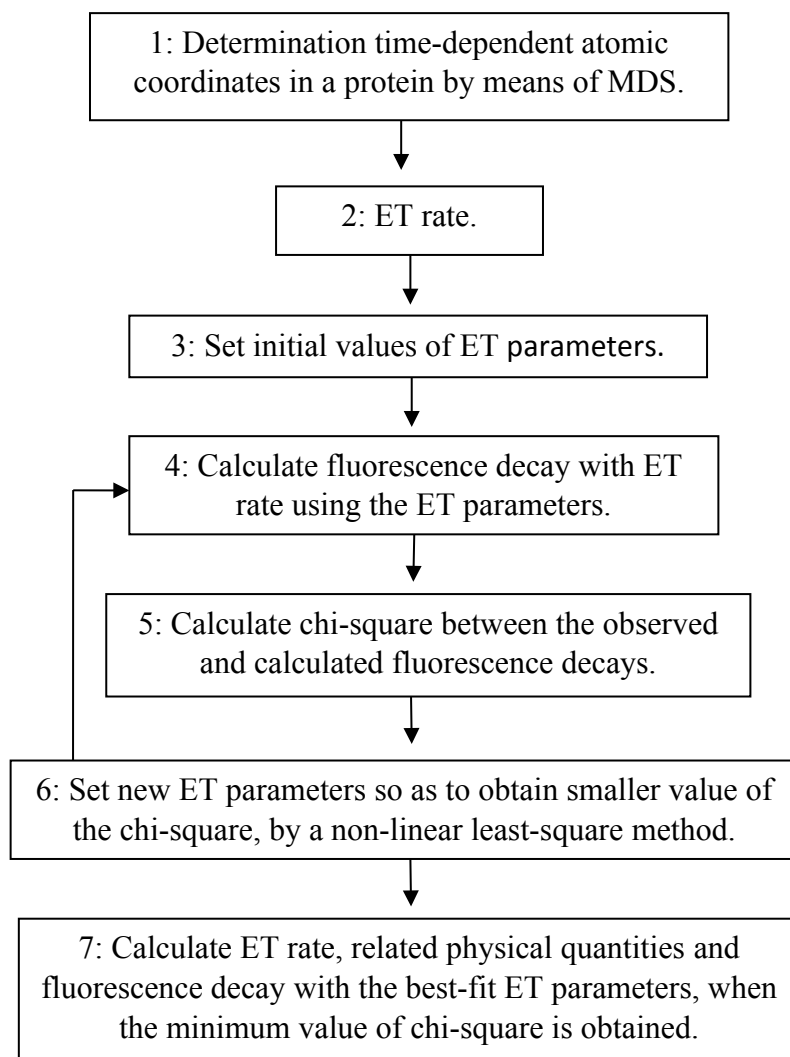


Diagram for procedure of ET analysis



(Data were taken from Ref 47).

ET rates from Trp168 to Iso* in P2OD³⁸ (References are listed in text)

ET rate of the fast component by KM model is expressed by eq S1.

$$k_{ij}^f = \frac{\nu_0^f}{1 + \exp\{\beta^f (R_i - R_0^f)\}} \sqrt{\frac{k_B T}{4\pi\lambda_S^f}} \exp\left[-\frac{\{\Delta G_{ij}^0 - e^2 / \varepsilon_{DA}^f R_i + \lambda_S^f + E_{Net}^f\}^2}{4\lambda_S^f k_B T}\right] \quad (\text{S1})$$

The P2O monomer contains 9 Trp and 15 Tyr residues. In the present work the ET rate only from Trp168 in each subunit was taken into account among these aromatic amino acids, because the Trp168-Iso distance is within 0.8 nm in all subunits, while those of other aromatic amino acids are longer than 1.2 nm⁴⁸ (see Table S1, Supporting Information). In eq. S1 k_{ij}^f is an ET rate of the fast component from Trp168 to the Iso* in subunit i at the emission wavelength j . ν_0^f is an adiabatic frequency, β^f is the ET process coefficient of the fast component. R_i and R_0^f are Trp168–Iso distance in subunit i and its critical distance for the ET process of the fast component, respectively. R_i is expressed as a center-to-center distance (R_c), because Marcus theory⁴⁹⁻⁵¹ and the following ET theories⁵²⁻⁵⁷ were derived assuming the donor and acceptor molecules to be spherical. The ET process is adiabatic when $R_i \leq R_0^f$, and non-adiabatic when $R_i > R_0^f$. The term, $-e^2 / \varepsilon_{DA}^f R_i$, in eq. S1 is electrostatic (ES) energy between Iso anion and a donor cation (*ESDA*), where ε_{DA}^f is static dielectric constant near Trp168 and Iso in the fast component. The k_B , T, and e are Boltzmann

constant, temperature and electron charge, respectively. E_{Net}^{if} is a net ES energy (*NetES*) of Trp168 in subunit i for the fast component, which is described later. λ_S^{if} is the solvent reorganization energy^{49,50} (*SROE*) of the ET donor in subunit i for the fast component, and is expressed as eq. S2.

$$\lambda_S^{if} = e^2 \left(\frac{1}{2a_{Iso}} + \frac{1}{2a_{Trp}} - \frac{1}{R_i} \right) \left(\frac{1}{\epsilon_\infty} - \frac{1}{\epsilon_{DA}^f} \right) \quad (S2)$$

where a_{Iso} and a_{Trp} are the radii of Iso and Trp, with these reactants being assumed to be spherical, and ϵ_∞ is optical dielectric constant. The optical dielectric constant used was 2.0. The radii of Iso (a_{Iso}) and Trp (a_{Trp}) were those previously determined³⁰⁻³⁸ to be 0.224 and 0.196 nm, respectively.

The standard free energy gap (*SFEG*) for fast component was expressed with the ionization potential of Trp, E_{IP} , as eq. S3.

$$\Delta G_{ff}^0 = E_{IP} - G_{ff}^0 \quad (S3)$$

Here G_{ff}^0 is the standard Gibbs energy related to the electron affinity of Iso* in the fast component at emission wavelength j . The experimental value of E_{IP} for Trp is 7.2 eV.⁶⁴ In the present work we assumed the emission-wavelength dependence of ET rate with the emission-wavelength dependent G_{ff}^0 , because G_{ff}^0 is related to the electronic energy of Iso*, and further it depends on hydrogen bonding (H-bond) between Iso* and surrounding amino acids.^{60,61}

ET rate for the slow component was expressed by eq. S4

$$k_i^s = \frac{\nu_0^s}{1 + \exp\{\beta^s (R_i - R_0^s)\}} \sqrt{\frac{k_B T}{4\pi\lambda_S^{is}}} \exp\left[-\frac{\{\Delta G_s^0 - e^2 / \epsilon_{DA}^s R_i + \lambda_S^{is} + E_{Net}^{is}\}^2}{4\lambda_S^{is} k_B T}\right] \quad (S4)$$

ν_0^s is an adiabatic frequency, β^s the ET process coefficient and R_0^s the critical distance for slow component. λ_S^{is} is the *SROE* in the slow component, given by eq. S5.^{49,50}

$$\lambda_S^{is} = e^2 \left(\frac{1}{2a_{Iso}} + \frac{1}{2a_{Trp}} - \frac{1}{R_i} \right) \left(\frac{1}{\epsilon_\infty} - \frac{1}{\epsilon_{DA}^s} \right) \quad (S5)$$

ΔG_s^0 is *SFEG* of the slow component between the products and reactants, as expressed by eq. S6

$$\Delta G_s^0 = E_{IP} - G_s^0 \quad (S6)$$

G_s^0 is the free energy related to electron affinity of Iso* in the slow component. The other variables and constants in eq. S4 are similar with those in eq. S1.

Electrostatic energy in P2O tetramer

Ionic groups in a flavoprotein could influence the ET rate. The FAD cofactor has two negative charges at the pyrophosphate, whilst P2O itself contains 34 Glus, 37 Asps, 26 Lyss and 27 Args residues per subunit. Therefore total numbers of ionic groups are four times of those in a subunit. The ES energy between the Iso anion or Trp168 cation and all other ionic groups in subunit i of the component c is expressed by eq. S7.

$$E_j^{ci} = \sum_{l=1}^4 \sum_{k=1}^{34} \frac{C_j \cdot C_{Glu}}{\epsilon_0^c R_{li}^c (Glu - k)} + \sum_{l=1}^4 \sum_{k=1}^{37} \frac{C_j \cdot C_{Asp}}{\epsilon_0^c R_{li}^c (Asp - k)} \\ + \sum_{l=1}^4 \sum_{k=1}^{26} \frac{C_j \cdot C_{Lys}}{\epsilon_0^c R_{li}^c (Lys - k)} + \sum_{l=1}^4 \sum_{k=1}^{27} \frac{C_j \cdot C_{Arg}}{\epsilon_0^c R_{li}^c (Arg - k)} + \sum_{l=1}^4 \sum_{k=1}^4 \frac{C_j \cdot C_P}{\epsilon_0^c R_{li}^c (P - k)} \quad (S7)$$

Here $j = 0$ for the Iso anion in subunit i , 1 for the Trp168 cations. The component c is f for the fast component and s for the slow component. C_j is the charge of the aromatic ionic species j , that is, $-e$ for $j = 0$ and $+e$ for $j = 1$. C_{Glu} ($= -e$), C_{Asp} ($= -e$), C_{Lys} ($= +e$), and C_{Arg} ($= +e$) are the charges of the Glu, Asp, Lys and Arg residues, respectively. FAD contains 2 phosphate atoms, each of which binds 2 oxygen atoms. It was assumed that the charge of each oxygen atom is $C_p = -0.5e$ (total charge of four oxygen atoms is $-2e$). All the measurements were performed at pH 7.0. We also assumed that these groups are all in an ionic state in solution at pH 7.0 since the pK_a values of these amino acids in water are 4.3 in Glu, 3.9 in Asp, 10.5 in Lys, and 12.5 in Arg. Histidine (His) has a pK_a of 6.0 in water. In protein the pK_a varies from 5.5 to 6.7 (RNase A).⁶⁵⁻⁶⁷ Accordingly, His residues should be deprotonated and neutral. The positions of Glus and Asps were determined as center of two oxygen atoms of the side chain. The positions of Lyss were determined as N atoms of the side chains, and those of Args as center of two terminal N atoms. The distances between the aromatic ionic species j and the k^{th} Glu ($k = 1 - 44$) are denoted to be $R_j(Glu - k)$. The distances between the aromatic ionic species j and the

k^{th} Asp ($k = 1 - 37$) are denoted to be $R_j(\text{Asp} - k)$, and so on for other ionic amino acids. ε_0^c is a static dielectric constant of component c inside the subunits.

E_{Net}^{ci} in eqs. S1 and S4 was then expressed as eq. S8.

$$E_{Net}^{ci} = E_0^{ci} + E_1^{ci} \quad (\text{S8})$$

Experimental fluorescence decays of wild type P2O

The observed decay functions for the fast and the slow components are expressed by eqs. S9 and S10, respectively.

$$F_f(t\lambda_j) = \exp(-t / \tau_j^f) \quad (\text{S9})$$

$$F_s(t) = \exp(-t / \tau^s) \quad (\text{S10})$$

The observed decay parameters are listed in Table S2⁶² (Supporting Information). In eq. 9 $\tau_1^f = 0.092$ at $\lambda_1 = 580$ nm, $\tau_2^f = 0.113$ at $\lambda_2 = 555$ nm, $\tau_3^f = 0.110$ at $\lambda_3 = 530$ nm, $\tau_4^f = 0.070$ at $\lambda_4 = 500$ nm, $\tau_5^f = 0.057$ ps at $\lambda_5 = 480$ nm (mean 88 fs). The decay for the slow component is emission-wavelength independent. The value of the lifetime is $\tau^s = 358$ ps.

Calculated decay functions

The calculated decay functions of the fast components and slow component are expressed by eqs. S11 and S12, respectively.

$$F_{calc}^f(t\lambda_j) = \frac{1}{m} \sum_{i=1}^m \left\langle \exp \left[- \{k_{ij}^f(t')\} t \right] \right\rangle_{AV} \quad (m = 1 - 4, j = 1 - 5) \quad (S11)$$

$$F_{calc}^s(t) = \frac{1}{4-m} \sum_{i=1}^{4-m} \left\langle \exp \left[- \{k_i^s(t')\} t \right] \right\rangle_{AV} \quad (S12)$$

In eqs. S11 and S12 $k_{ij}^f(t')$ and $k_i^s(t')$ are MDS time (t')-dependent because the donor-acceptor distances and E_{Net}^i depend on t' , though the ET rates given by eqs. S1 and S4 are time-independent. $F_{calc}^f(t\lambda_j)$ in eq. S11 depends on the emission-wavelength λ_j ($j=1-5$). In the present model it was assumed that m subunits among 4 subunits display fast decay, and $4-m$ subunits, slow decay. In eq. S12 $F_{calc}^s(t)$ is the decay function of the slow component and independent of the emission wavelength.

When $m=1$, there should be four possible fast decays (each 5 decays with λ_j), namely i =SubA, Sub B, Sub C and Sub D. In the case that Sub A is fast component, Sub B, Sub C and Sub D are slow components. In the case that Sub B is fast component, Sub A, Sub C and Sub D are slow components. Likewise, in the case that Sub C is fast, Sub A, Sub B and Sub D are slow components, and in the case that Sub D is fast component, Sub A, Sub B and Sub C are slow components. When $m=2$, there should be six combinations of $F_{calc}^f(t\lambda_j)$ and $F_{calc}^s(t)$. If Sub A and Sub B are fast components, then Sub C and Sub D should be slow components, and so on. When $m=3$, there should be four possible combinations of $F_{calc}^f(t\lambda_j)$ and $F_{calc}^s(t)$, namely, Sub B, Sub C and Sub D are fast components (Sub A is slow component). Accordingly there are altogether 14 sets of $F_{calc}^f(t\lambda_j)$ and $F_{calc}^s(t)$ (see Table S3; Supporting Information).

The fluorescence decays were calculated up to 0.6 ps with 0.0012 ps time intervals for the fast decays and 500 ps with 1 ps time intervals for the slow decays. Note that $\langle \dots \rangle_{AV}$ denotes the averaging procedure of the exponential functions in eq. S11 and eq. S12 over MDS time t' . The averaging procedures were performed up to 5 ns with 0.2 ps time intervals over 25000 snapshots.³⁸

Determination of the ET parameters

Initially the ET parameters related to the electronic coupling term (ν_0^c , β^c and R_0^c) of Trp168 for both the fast and slow components were taken from those reported values in FBP.³⁴ In this model the unknown ET parameters were G_{ff}^0 ($\lambda_j; j=1-5$), G_s^0 (for slow component; λ -independent), ε_0^c ($c=f$ and s), and ε_{DA}^c ($c=f$ and s). Fitting between the observed and calculated decays, however, were not good enough. Accordingly, ν_0^c , β^c and R_0^c ($c=f$ and s) for Trp168, were added as unknown parameters. Therefore, the unknown ET parameters were altogether 16, ν_0^c , β^c and R_0^c ($c=f$ and s), G_{ff}^0 ($\lambda_j; j=1-5$), G_s^0 , ε_0^c ($c=f$ and s), and ε_{DA}^c ($c=f$ and s). These parameters were varied so as to obtain the minimum value of total chi-square expressed by eq. S13.

$$\chi_T^2(n) = \sum_{j=1}^5 \chi_{fn}^2(\lambda_j) + \chi_{sn}^2 \quad (\text{S13})$$

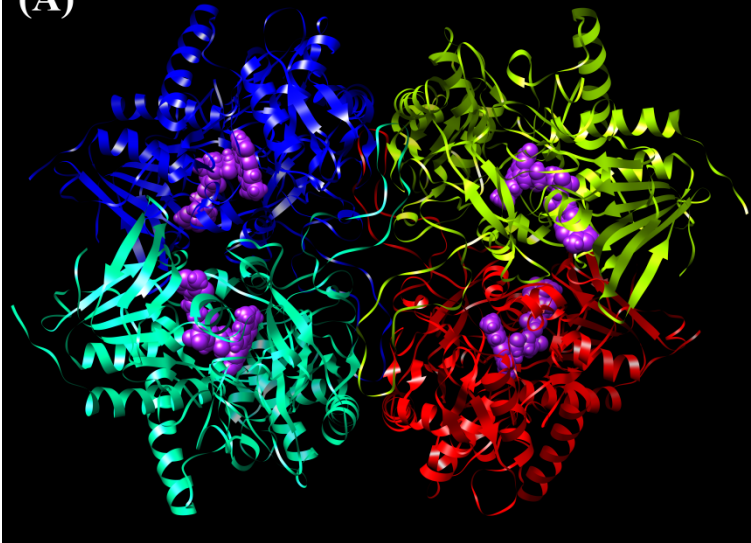
Here

$$\chi_{fn}^2(\lambda_j) = \frac{\{F_{calc}^f(t\lambda_j) - F_f(t\lambda_j)\}^2}{F_{calc}^f(t\lambda_j)} \quad (\text{S14})$$

$$\chi_{sn}^2 = \frac{\{F_{calc}^s(t) - F_s(t)\}^2}{F_{calc}^s(t)} \quad (\text{S15})$$

$\chi_T^2(n)$ is total chi-square of n -th combination as shown in Table S3 (Supporting Information). $\chi_{fn}^2(\lambda_j)$ and χ_{sn}^2 are chi-squares of the fast component at emission wavelength λ_j and the slow component for n -th combination of $F_{calc}^f(t\lambda_j)$ and $F_{calc}^s(t)$, respectively. ET rates and other physical quantities were calculated with the best-fit ET parameters.

(A)



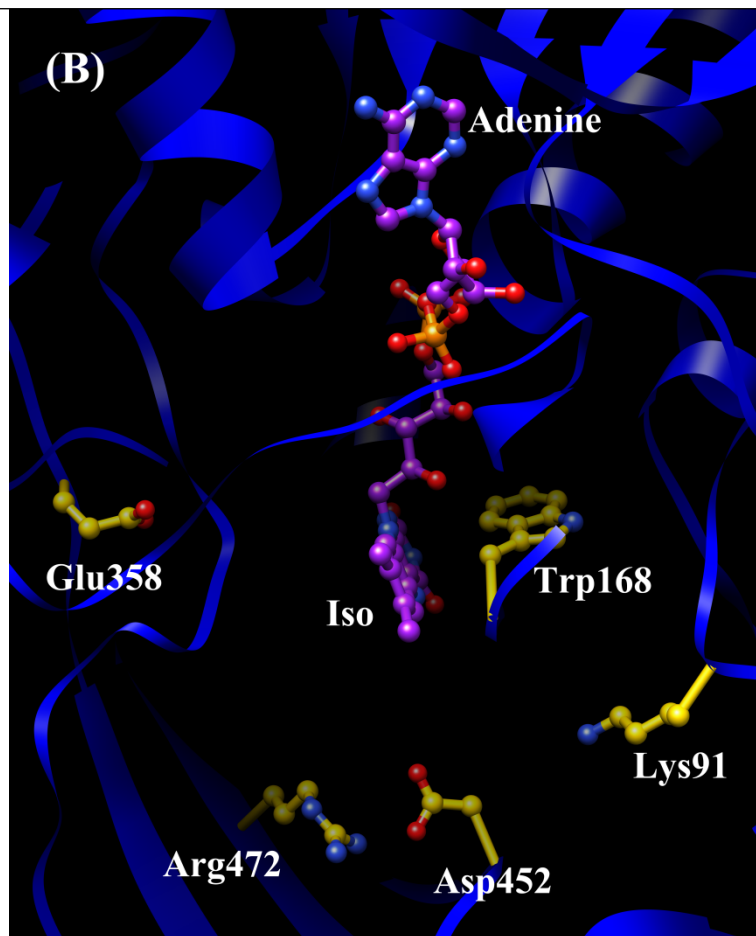
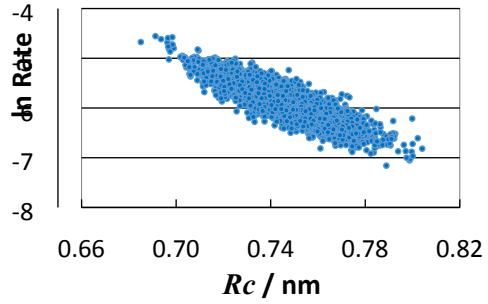


Figure S1 The three-dimensional structure and local structures near Iso of P2O.

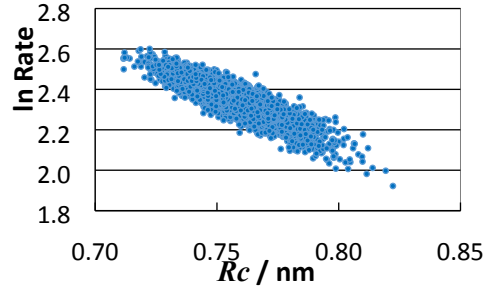
The panel (A) shows whole structure of the tetrameric protein, blue for subunit-A, green for

subunit-B, yellow for subunit-C and red for subunit-D, respectively. FAD molecules in the tetramer is indicated with the magenta stick models. The panel (B) shows the FAD binding site including the Trp168 and ionic amino acids. Data were taken from Ref 48.

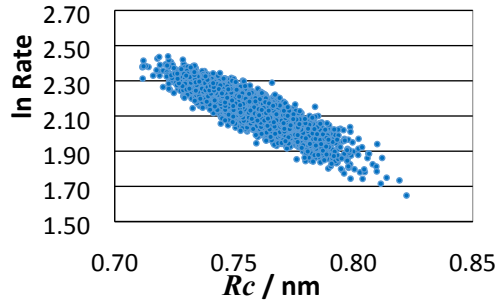
Slow: Sub A



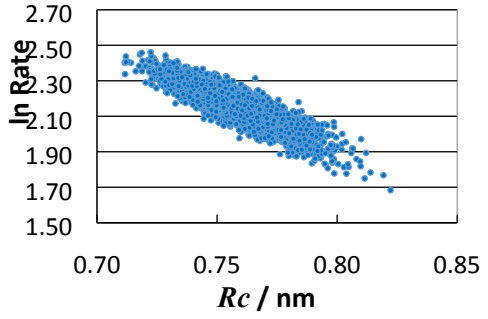
Fast: Sub C (580 nm)



Fast: Sub C (555 nm)



Fast: Sub C (530 nm)



Fast: Sub C (500 nm)

Fast: Sub C (480 nm)

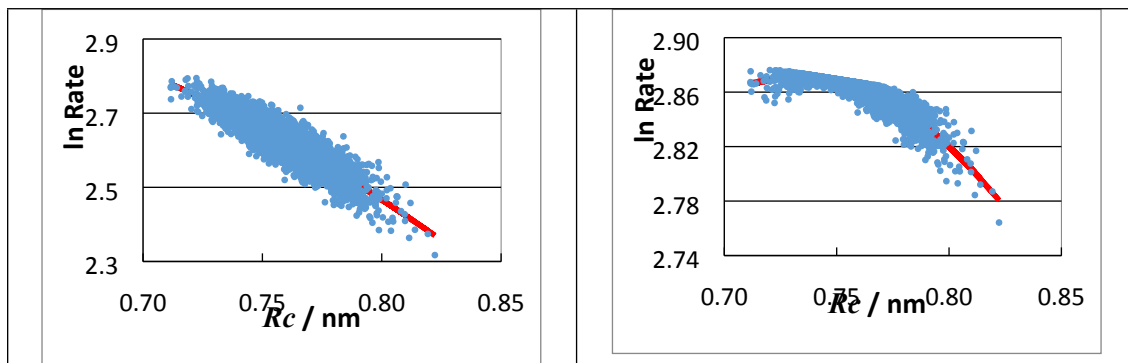


Figure S2 Relationship between ln Rate and R_c of Sub A and Sub C in wild type P2O.

Panel title, Slow: Sub A, denotes the slow component of Sub A. Panel titles of the other Figures denote fast component, subunit and emission wavelength in parentheses. Inserts indicate approximation functions of logarithmic ET rate vs R_c . The coefficients of the functions are listed in Table 6. Data were taken from Ref. 38.

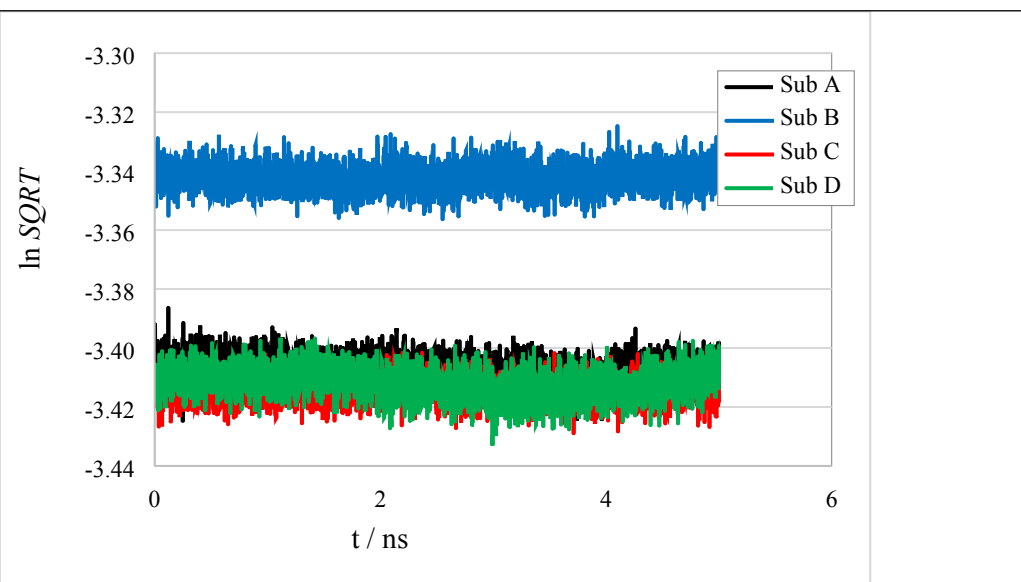
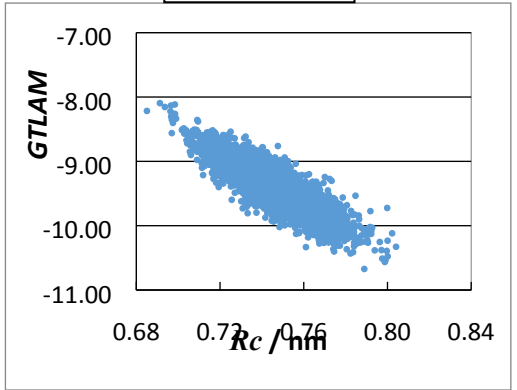


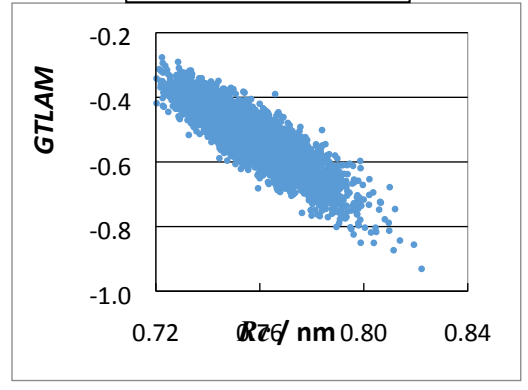
Figure S3 Dynamics of logarithmic $SQRT$ in P2O tetramer.

The $\ln SQRT$ is defined by eq. 3 in text. Insert denotes the subunits. Data were taken from Ref 38.

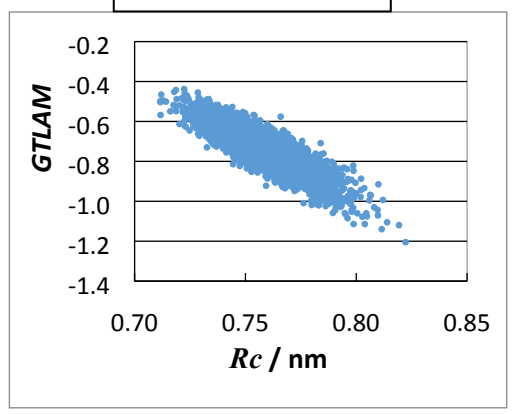
Slow: Sub A



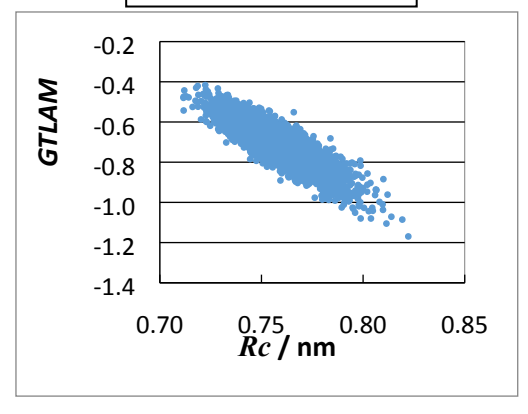
Fast: Sub C 580 nm



Fast: Sub C 555 nm



Fast: Sub C 530 nm



Fast: Sub C 500 nm

Fast: Sub C 480 nm

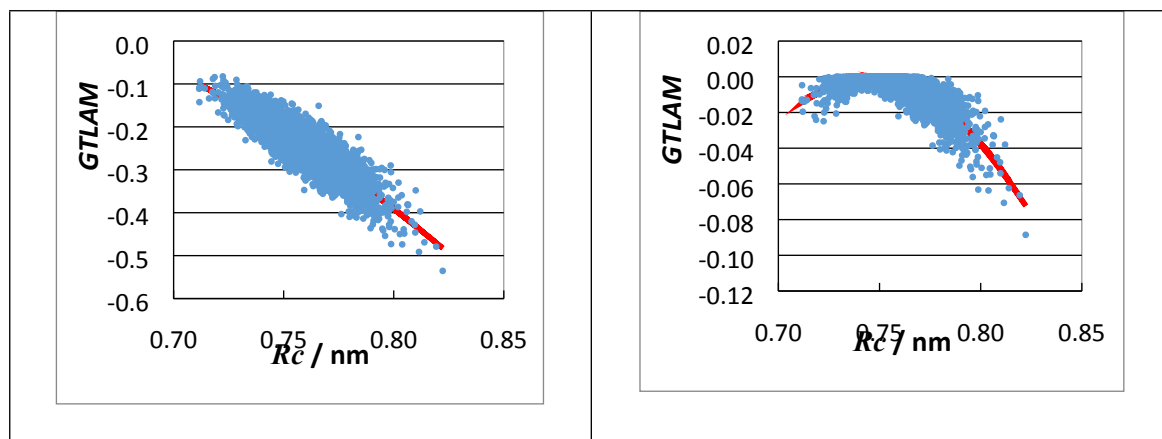


Figure S4 Relationship between $GTLAM$ and Rc in Sub A and Sub C in P2O.

Slow Sub A denotes the slow component Sub A. Panel titles of the other Figures denote fast component, subunit and emission wavelength in parentheses. Inserts indicate approximate functions of $GTLAM$ rate vs Rc . The coefficients of the functions are listed in Table S6. Data were taken from Ref 38.

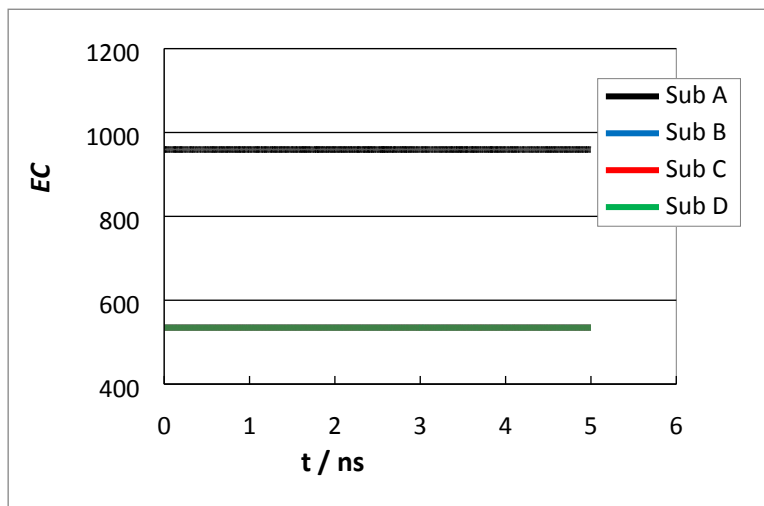


Figure S5 Time-evolution of EC in P2O.

EC denotes electronic coupling term, and is expressed in unit of ps^{-1} . The logarithmic EC is given by eq. 2 in text. Insert shows subunits. The values of EC were almost constant with time. The EC values were almost identical among the fast subunits, Sub B, Sub C and Sub D. Data were taken from Ref 38.

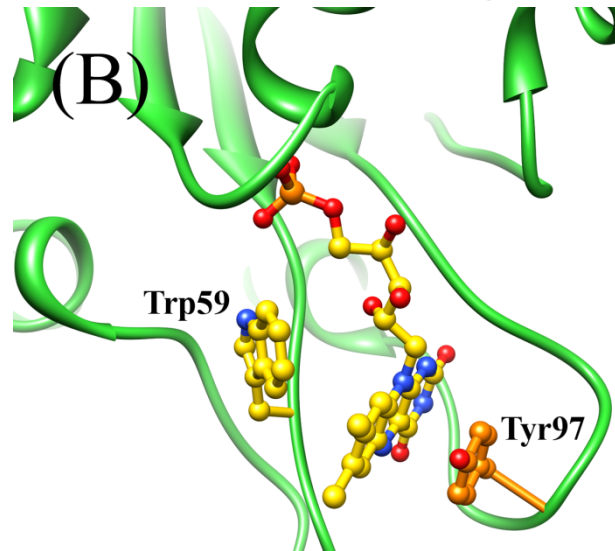
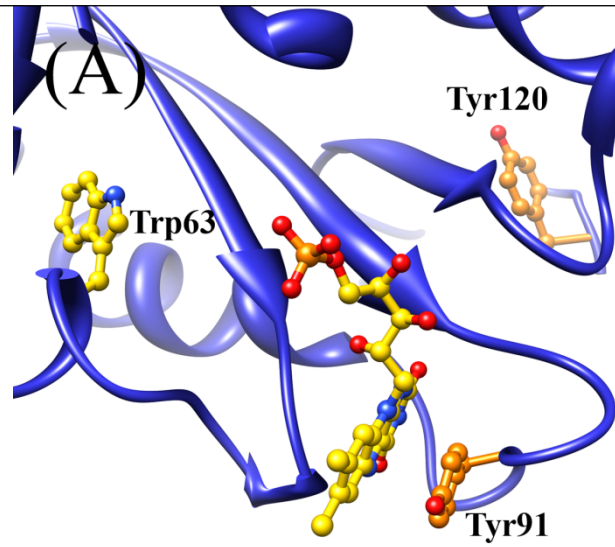


Figure S6 The protein structures near Iso binding site in HPFD and flavodoxin from *Desulfovibrio vulgaris* (MF) obtained by MDS

Panel (A) shows HPFD, where Iso is stacked with Tyr91. Panel (B) shows flavodoxin from *Desulfovibrio vularis* (Miyazaki F) (DVFD), where it is sandwiched by Trp59 and Tyr97. Mean distance (R_c) between Iso and Tyr91 is 0.56 nm, which are similar to those of R_c between Iso and Tyr97 in DVFD. Data were taken from Ref 35.

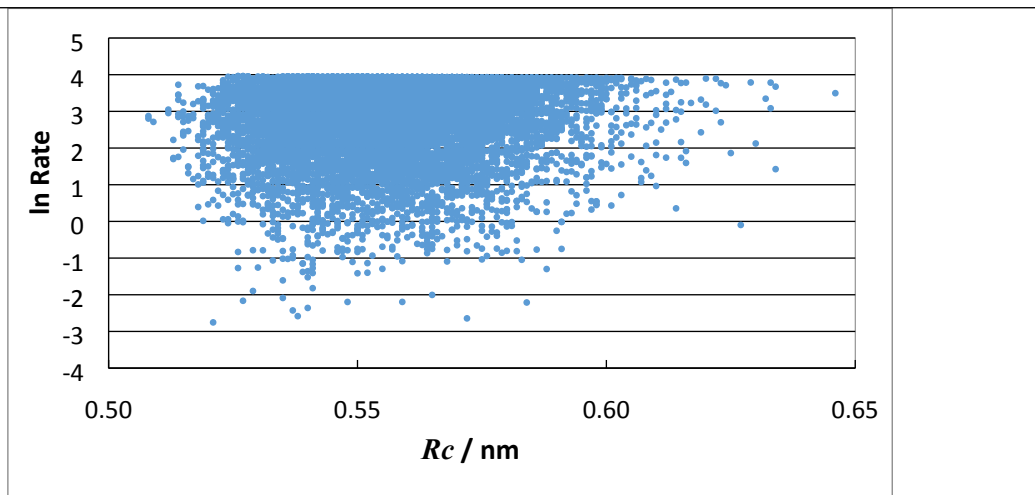
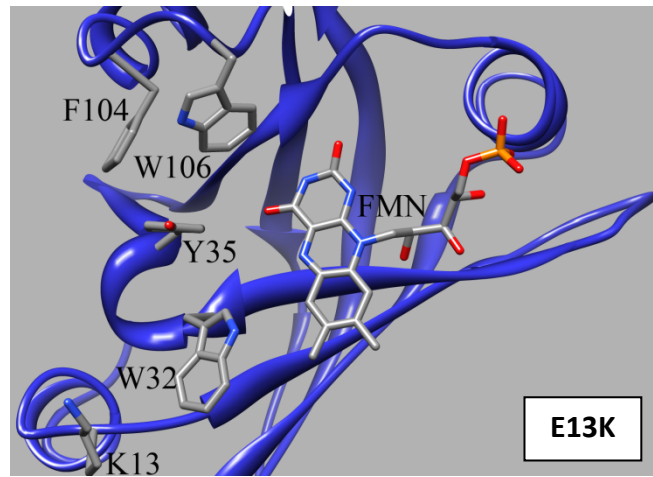
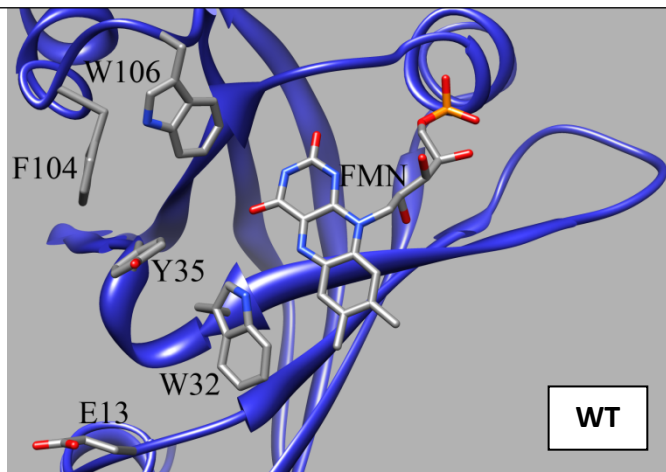
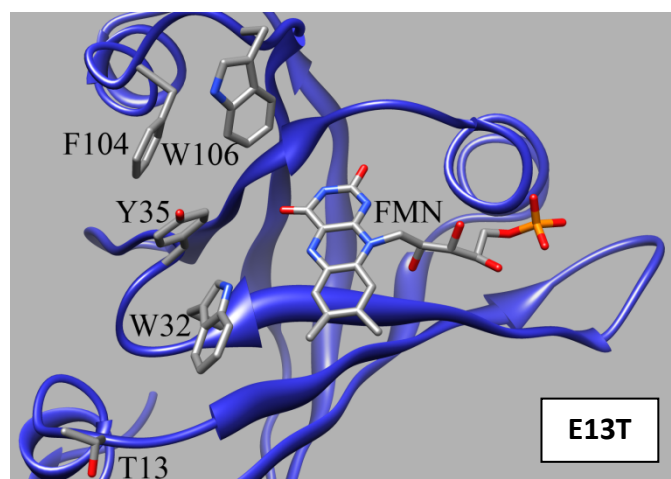
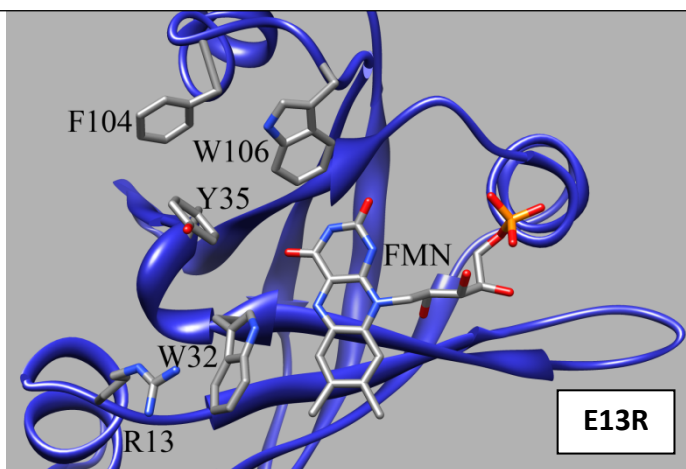


Figure S7 Relationship between $\ln \text{Rate}$ and R_c in HPFD

No clear relation between $\ln \text{Rate}$ and R_c is found. Data were taken from Ref 35.





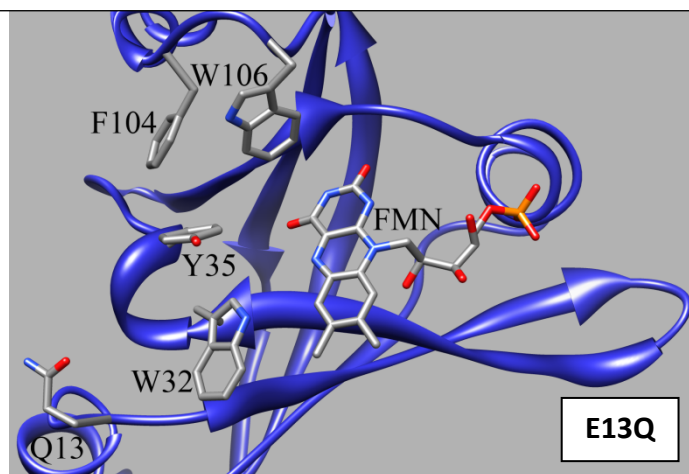
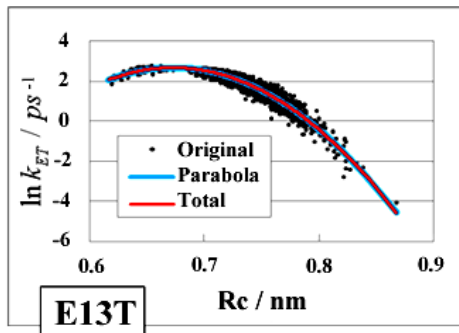
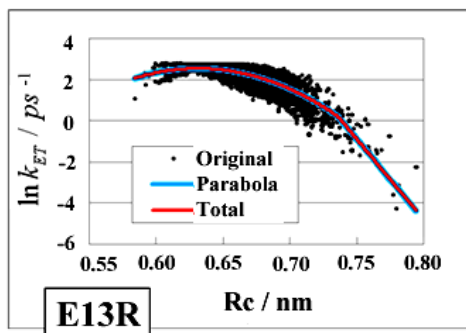
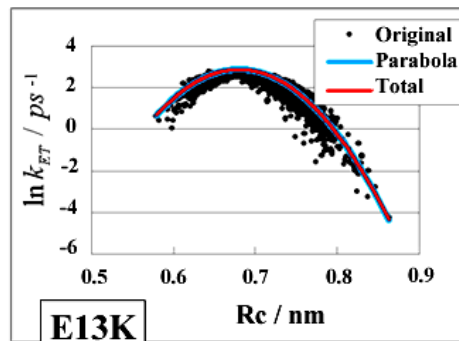
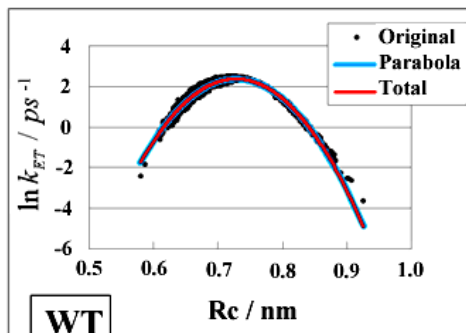


Figure S8 Protein structures near FMN binding sites of five FBP isoforms obtained by MDS snapshots.

W32 (Trp32), Y35 (Tyr35), W106 (Trp106) are potential ET donors. Glu13 (E13) in WT FBP is replaced by Lys13 in E13K, by Arg13 in E13R, by Thr13 in E13T, and Gln13 in E13Q. Data were taken from Ref 37.



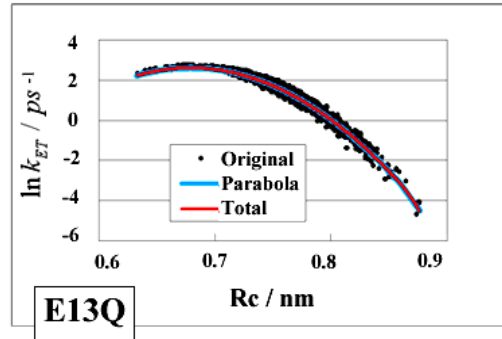


Figure S9 Dependence of logarithmic ET rates on Rc of Trp32 in five FBP isoforms.

Inserts indicate, Original: original ET rates obtained with KM rates, Parabola: the original ET rates are approximated with parabolic functions, and Total: the original ET rates are approximated with a parabolic function at Rcs shorter than a certain value (D_0) dependent on the isoform, plus linear function at Rcs longer than D_0 . Data were taken from Ref. 36.

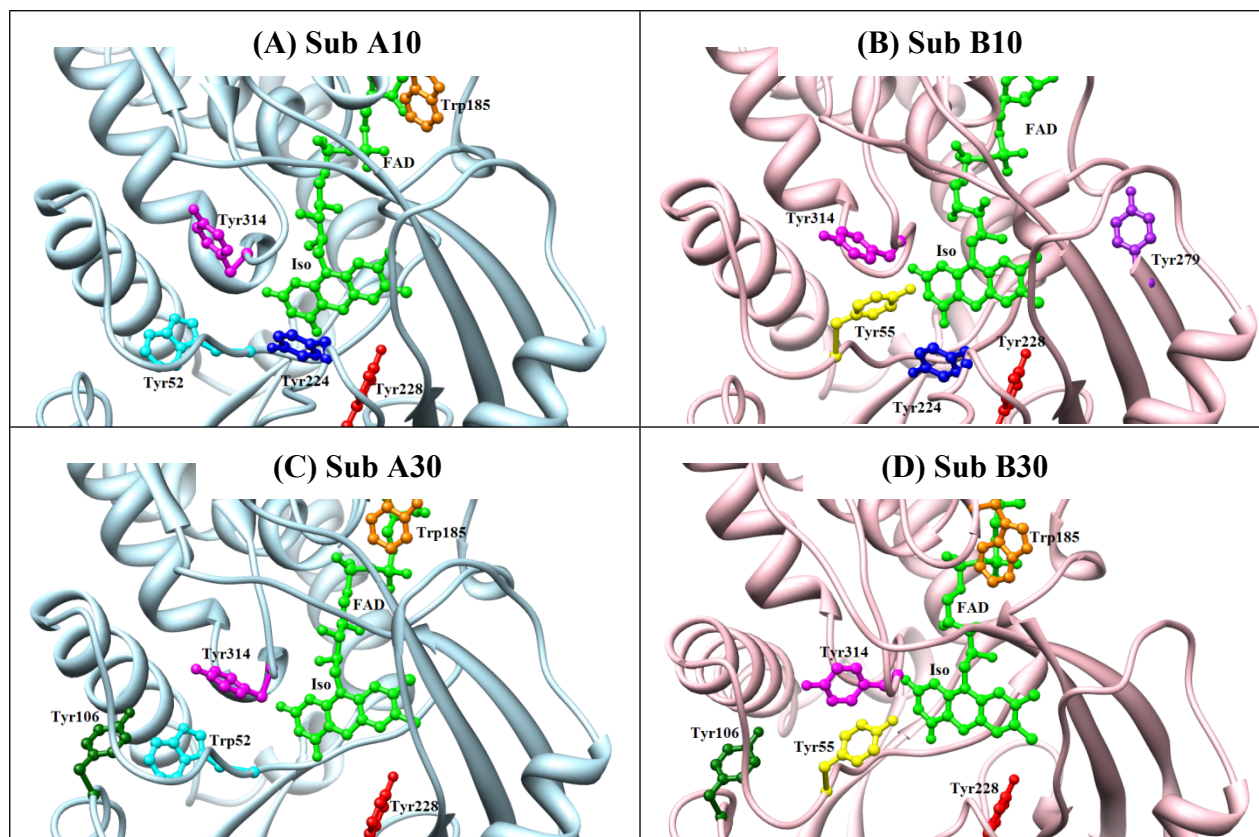


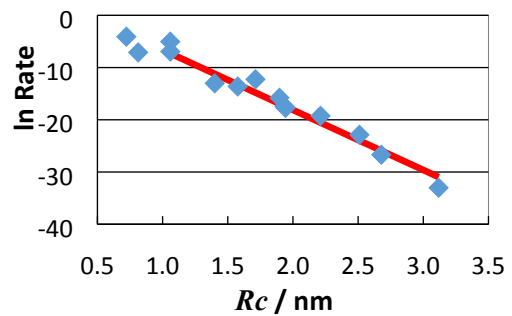
Figure S10 Local structure of FAD binding site in DAAO dimer from porcine kidney

obtained by MDS.

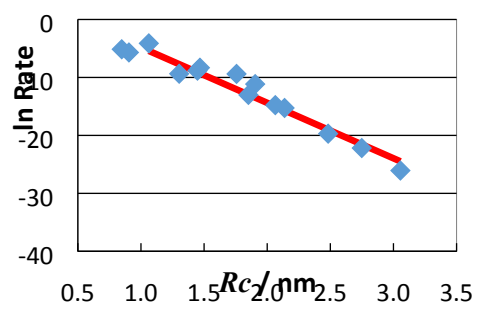
The five fastest ET donors are illustrated with stick model, together with FAD. Sub A10 and Sub B10 denote subunits of A and B at 10 °C, and Sub A30 and Sub B30 denote subunits of A and B at 30 °C. MDS calculations were performed independently both at 10 °C and 30 °C. Data

were taken from Ref. 60.

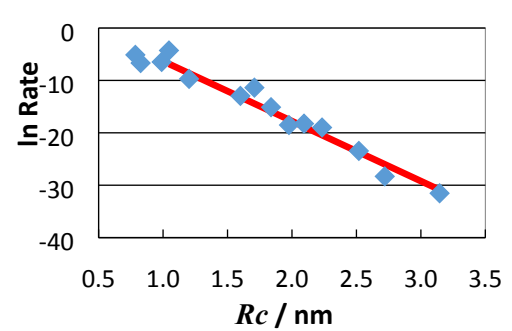
Sub 10A



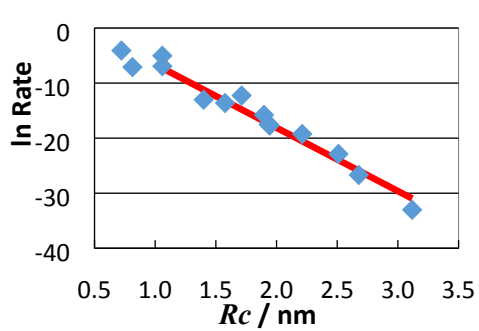
Sub 30A



Sub 10B



Sub 30B



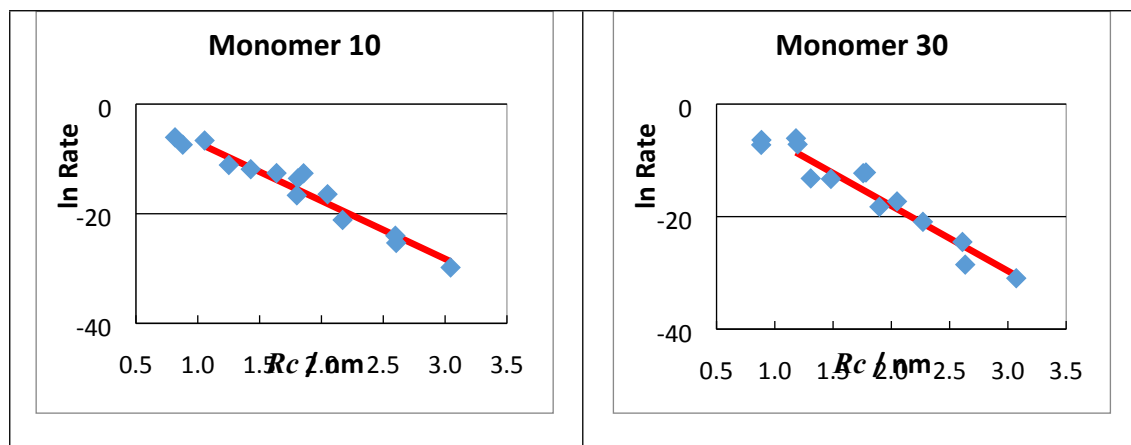


Figure S11 Dependence of logarithmic ET rates on R_c of Tyr as ET donor in DAAO dimer.

All Tyr as the donors in DAAO dimer are taken into account. Sub 10A and Sub 10B denote subunit A and subunit B of DAAO dimer at 10 °C, respectively. Sub 30A and Sub 30B denote subunit A and subunit B at 30 °C, respectively. Inserts indicate approximate linear functions. The $\ln \text{Rate}$ vs R_c relation for the monomer of DAAO is also shown for comparison. Data were taken from Ref 60.

Table S1 R_c between Iso and nearby aromatic amino acids in wild type P2O^a

Subunit	Trp168	Trp253	Tyr456	Tyr590	Tyr199	Tyr96
A	0.746 (0.614)	1.35 (1.12)	1.52 (1.11)	1.22 (1.27)	1.70	1.92
B	0.731 (0.616)	1.28 (1.12)	2.21 (1.12)	1.27 (1.25)	1.71	1.69
C	0.758 (0.611)	1.33 (1.12)	2.08 (1.10)	1.29 (1.27)	1.72	1.75
D	0.749 (0.611)	1.31 (1.12)	1.96 (1.11)	1.26 (1.26)	1.70	1.73

^a Mean values in unit of nm are listed over 25000 snapshots with 0.2 ps time intervals. The distances in parentheses were obtained using the crystal structure of P2O. Data were taken from Ref 48.

Table S2 Experimental fluorescence lifetime of wild type P2O^a

Wavelength (nm)	τ_i^f (fs)	τ^s (ps)	α_i^f	α^s
580	92	358	0.88	0.12
555	113	358	0.85	0.15
530	110	358	0.81	0.19
500	70	358	0.95	0.05
480	57	358	0.99	0.01

^a τ_i^f and τ^s are the lifetime of the fast component at the emission wavelength i , and of the slow component, respectively. α_i^f and α^s are their component fractions. Data were taken from Ref 62.

Table S3 Chi-square for all possible combinations of the fast and slow subunits among the four subunits in P2O^a

Case (<i>n</i>)	Subunit				$\chi^2_T(n)$
	Sub A	Sub B	Sub C	Sub D	
1	Slow	Fast	Fast	Fast	2.63×10^{-5}
2	Fast	Slow	Fast	Fast	6.50×10^{-1}
3	Fast	Fast	Slow	Fast	3.55×10^{-4}
4	Fast	Fast	Fast	Slow	3.47×10^{-4}
5	Fast	Slow	Slow	Slow	5.83×10^{-1}
6	Slow	Fast	Slow	Slow	3.42×10^{-1}
7	Slow	Slow	Fast	Slow	3.34×10^{-2}
8	Slow	Slow	Slow	Fast	4.02×10^{-1}
9	Slow	Slow	Fast	Fast	3.33×10^{-2}
10	Slow	Fast	Slow	Fast	6.79×10^{-1}
11	Slow	Fast	Fast	Slow	6.82×10^{-1}
12	Fast	Slow	Slow	Fast	3.33×10^{-2}
13	Fast	Slow	Fast	Slow	3.33×10^{-2}

14 Fast Fast Slow Slow 3.37×10^{-2}

a $\chi_T^2(n)$ is given by eq. S13, and were evaluated for all possible combinations of $F_{calc}^{fi}(t)$ and $F_{calc}^s(t)$ [see eqs. S11 and S12 above]. The value of $\chi_T^2(n)$ was smallest when Sub A is the slow component, and Sub B, Sub C and Sub D are the fast component. Data were taken from Ref 38.

Table S4 Determined standard free energy related to electron affinity of Iso* in P2O^a

Fluorescent component	λ_j (nm)	G_{ff}^0 ^b (G_s^0 ^c) (eV)	ΔG_{ff}^0 ^b (ΔG_s^0 ^c) (eV)	$\chi_{fn}^2(\lambda_j)$ ^d (χ_{sn}^2 ^e)
Fast	580	8.59	-1.39	2.14×10^{-5}
	555	8.53	-1.33	3.45×10^{-5}
	530	8.54	-1.34	3.30×10^{-5}
	500	8.70	-1.50	4.88×10^{-6}
	480	8.89	-1.69	1.32×10^{-7}
Slow	530	(7.33)	(-0.13)	(6.36×10^{-5})

a Total value of chi-square, $\chi_T^2(n)$, given by eq. S13 was 2.63×10^{-5} (see Table 1). Data were taken from Ref 38.

b Given by eq. S3.

c Given by eq. S6.

d Given by eq. S14.

e Given by eq. S15.

Table S5 Best-fit ET parameter in the electronic coupling term and the static dielectric constant in P2O^a

ν_0^f	β^f	R_0^f	ν_0^s	β^s	R_0^s	ϵ_0^f	ϵ_0^s	ϵ_{DA}^f	ϵ_{DA}^s
535	21.0	1.30	959	20.8	1.21	11.4	10.8	9.78	5.76

f and s denote fast and slow components. Definitions of these parameters are given below eq. S1 and eq S4. ϵ_0^c is the static dielectric constant of component c inside the subunits, and ϵ_{DA}^c the static dielectric constant of c near Iso and Trp168. Data were taken from Ref 38.

Table S6 Physical quantity dependent on the emission wavelength in P2O^a

Component	Wavelength (nm)	Subunit	GT^b (eV)	$GTRAM^c$	Rate ^d (ps ⁻¹)	ln Rate
Fast	580 nm	Sub B	0.266	-0.381	12.1	2.50
		Sub C	0.315	-0.526	10.4	2.35
		Sub D	0.311	-0.514	10.6	2.36
	555 nm	Sub B	0.324	-0.566	10.1	2.31
		Sub C	0.374	-0.739	8.44	2.13
		Sub D	0.369	-0.726	8.59	2.15
	530 nm	Sub B	0.317	-0.541	10.4	2.34
		Sub C	0.367	-0.711	8.68	2.16
		Sub D	0.362	-0.698	8.83	2.18
	500 nm	Sub B	0.163	-0.145	15.3	2.73
		Sub C	0.212	-0.240	13.9	2.63
		Sub D	0.208	-0.232	14.0	2.64
480 nm	Sub B	-0.0294	-0.00880	17.6	2.87	

	Sub C	0.0201	-0.00561	17.5	2.86
	Sub D	0.0157	-0.00551	17.5	2.86
Slow	Sub A	1.24	-9.40	0.00296	-5.82

a Mean values are obtained over 25000 snapshots with 0.2 ps intervals. Standard free energy (G_{fi}^0 and G_s^0) and standard free energy gap (ΔG_{fi}^0 and ΔG_s^0) are listed in Table S4. Data were taken from Ref 38.

b Total free energy gap given by eq. 4 in text.

c Exponential term of the ET rate defined by eq. 5 in text.

d The rate for the fast component is given by eq. S1 above, and for the slow component by eq. S4.

Table S7 Coefficients in approximation functions of \ln Rate vs Rc plot and of $GTLAM$ vs Rc plot in P2O ^a

Subunit	Wavelength (nm)	Coefficient					
		\ln Rate vs Rc^b			$GTLAM$ vs Rc^c		
		A	B	C	A	B	C
Sub A	-	-18.28	7.76	-	-18	4.04	-
Sub B	580	-4.61	5.87	-	-5.23	3.26	-
	555	-5.51	6.33	-	-5.51	6.33	-
	530	-5.4	6.28	-	-5.12	3.21	-
	500	-10.5	12.4	-0.723	-10.9	13.3	-4.03
	480	-13	19.2	-4.24	-13.4	20.13	-7.55
Sub C	580	-5.11	6.22	-	-5.7	3.58	-
	555	-5.95	6.64	-	-5.95	6.64	-
	530	-5.85	6.59	-	-5.6	3.53	-
	500	-7.3	7.51	1.13	-7.68	8.34	-2.15
	480	-11.6	17	-3.38	-11.99	17.87	-6.66

Sub D	580	-4.61	5.81	-	-4.36	2.75	-
	555	-5.37	6.17	-	-5.12	3.11	-
	530	-5.28	6.13	-	-5.02	3.07	-
	500	-3.48	2	3.09	-3.88	2.86	-0.194
	480	-9.37	13.6	-2.05	-9.77	14.44	-5.34

a Linear functions are expressed by $Y = A X + b$, and parabolic functions $Y = A X^2 + B X + C$. Data were taken from Ref 38.

b $Y = \ln \text{Rate}$, and $X = Rc$

c $Y = GTLAM$, and $X = Rc$.

Table S8 ET rate and physical quantity related to ET rate in HPFD^{a)}

Rate ^{b)} (ps ⁻¹) (ln Rate)	<i>NetES</i> ^{c)} (eV)	<i>ESDA</i> ^{d)} (eV)	<i>SROE</i> ^{e)} (eV)
22.5 (3.11)	-0.117	-1.15	0.268

a Mean values over 50000 snapshots. $\Delta G_{\text{Tyr91}}^0$ (*SFEG*) corresponding to eqs. S3 or S6 in this Supporting Information for P2O is 0.841 eV in HPFD. Data were taken from Ref 35.

b ET rate from Tyr91 to Iso*.

c Net electrostatic energy between the photo-products and ionic groups in the protein.

d Solvent reorganization energy.

Table S9 Best-fit ET parameter in five FBPs^a

ν_0^{Trp} (ps ⁻¹)	ν_0^{Tyr} (ps ⁻¹)	β^{Trp} (nm ⁻¹)	β^{Tyr} (nm ⁻¹)	R_0^{Trp} (nm)	R_0^{Tyr} (nm)
161	204	31.9	6.24	0.770	1.00
ϵ_0^{WT}	ϵ_0^K	ϵ_0^R	ϵ_0^T	ϵ_0^Q	ϵ_0^{DA}
14.2	11.1	10.2	8.08	9.27	2.20
χ_{WT}^2	χ_K^2	χ_R^2	χ_T^2	χ_Q^2	χ_{Total}^2
1.22 x 10 ⁻³	1.88 x 10 ⁻³	1.52 x 10 ⁻³	2.88 x 10 ⁻³	2.68 x 10 ⁻³	2.04 x 10 ⁻³

^a Indexes WT, K, R, T, and Q for the static dielectric constant ϵ_0 and chi-square χ^2 denote WT, E13K, E13R, E13T and E13Q FBP isoforms,

respectively. The values of G_{Iso}^0 was 6.65 eV. Data were taken from Ref 37.

Table S10 ET rate in the five FBP isoforms^a

Donor		WT	E13K	E13R	E13T	E13Q
Trp32	Max ^b	10.7	14.4	15.3	14.9	14.4
	Av1 ^c	6.11	8.65	8.25	6.70	5.02
	Av2 ^d	7.02	10.2	9.75	8.27	6.57
Tyr35	Max ^b	1.12 x 10 ⁻¹⁸	3.68 x 10 ⁻¹⁷	1.64 x 10 ⁻²²	3.12 x 10 ⁻²²	6.78 x 10 ⁻¹⁷
	Av1 ^c	9.17 x 10 ⁻²⁰	9.19 x 10 ⁻¹⁸	1.48 x 10 ⁻²³	6.99 x 10 ⁻²³	2.87 x 10 ⁻¹⁷
	Av2 ^d	1.21 x 10 ⁻¹⁴	2.12 x 10 ⁻¹³	1.05 x 10 ⁻²⁰	3.50 x 10 ⁻¹⁷	1.53 x 10 ⁻¹⁴
Trp106	Max ^b	2.50 x 10 ⁻²	6.74 x 10 ⁻³	4.17 x 10 ⁻³	4.37 x 10 ⁻²	5.13 x 10 ⁻²
	Av1 ^c	9.89 x 10 ⁻⁴	4.53 x 10 ⁻³	4.57 x 10 ⁻³	3.31 x 10 ⁻²	3.80 x 10 ⁻²
	Av2 ^d	2.08 x 10 ⁻²	6.71 x 10 ⁻³	6.19 x 10 ⁻³	3.93 x 10 ⁻²	5.54 x 10 ⁻²

^a The ET rates from the donor (Trp32, Tyr35 and Trp106 are expressed in unit of ps⁻¹. Data were taken from Ref 37.

^b The ET rates at maximum distributions.

c Average rates were evaluated by integrations over the distributions of logarithmic rates.

d Average rates were evaluated by simple sums divided by number of logarithmic rates

Table S11 Physical quantity related to ET rate in five FBP isoforms^a

Protein	Donor	<i>SROE</i> ^b (eV)	<i>NetES</i> ^c (eV)	<i>ESDA</i> ^d (eV)	<i>SFEG</i> ^e (eV)	ln Rate ^f
WT	Trp32	0.220	0.0759	-0.935	0.548	1.81
	Tyr35	0.270	0.153	-0.650	1.35	-43.8
	Trp106	0.250	-0.0717	-0.627	0.548	-6.92
E13K	Trp32	0.219	0.198	-0.937	0.548	2.16
	Tyr35	0.259	0.207	-0.767	1.35	-39.2
	Trp106	0.243	-0.348	-0.700	0.548	-5.40
E13R	Trp32	0.214	0.309	-0.987	0.548	2.11
	Tyr35	0.268	0.276	-0.671	1.35	-52.6
	Trp106	0.243	-0.350	-0.702	0.548	-5.39

E13T	Trp32	0.223	0.224	-0.905	0.548	1.90
	Tyr35	0.260	0.334	-0.754	1.35	-51.0
	Trp106	0.241	-0.258	-0.717	0.548	-3.41
E13Q	Trp32	0.225	0.207	-0.876	0.548	1.61
	Tyr35	0.248	0.293	-0.876	1.35	-38.1
	Trp106	0.243	-0.201	-0.698	0.548	-3.27

a Mean values over MDS time range. Data were taken from Ref 37.

b Solvent reorganization energy.

c Net electrostatic (ES) energy.

d ES energy between Iso anion and Trp or Tyr cation.

e Standard free energy gap.

f The logarithmic ET rate.

Table S12 Best-fit ET parameter in DAAO dimer^a

T (°C)	Subunit	ϵ_0^{pk} ^b	$G_k^0(T)$ ^c (eV)	$\Delta G_k^0(T)$ ^d (eV)		τ (ps)		Chi-sq ^g
				(Trp)	(Tyr)	Obs ^e	Calc ^f	
10	Sub A	5.79	8.16	-1.41	-0.607	44.2	44.2	3.22 x 10 ⁻²⁸
	Sub B	5.82	8.54	-1.34	-0.536	-	-	7.47 x 10 ⁻²⁸
	Monomer ^h	5.88	8.69	-1.49	-0.69	228	228	-
30	Sub A	5.79	8.73	-1.53	-0.736	37.7	37.7	1.10 x 10 ⁻²⁵
	Sub B	5.82	8.48	-1.28	-0.481	-	-	2.16 x 10 ⁻²⁸
	Monomer ^h	5.89	8.51	-1.31	-0.48	182	182	-

a Data were taken from Ref 60.

b Static dielectric constants inside Sub A (ϵ_0^A) and inside Sub B.

c Temperature dependent standard free energy gap.

d Temperature-dependent electron affinity of Iso*.

e Reported fluorescence lifetimes. The lifetimes of Sub A and Sub B was not experimentally resolved.

f Calculated lifetimes.

g Chi-square between the observed and calculated lifetimes. Total Chi-square was 2.8 x 10⁻²⁶.

h ET parameters for monomer were taken from the reported work for comparison.⁶¹

Table S13 Physical quantity related to ET rate in

Subunit	Donor	ET rate	<i>NetES</i> ^b	<i>SROE</i> ^c	<i>ESDA</i> ^d	DAAO dimer ^a
(T / °C)		(ps ⁻¹)	(eV)	(eV)	(eV)	
A (10)	Tyr224	1.29 x 10 ⁻²	0.044	1.09	-0.331	
	Tyr314	7.57 x 10 ⁻³	-0.406	1.82	-0.224	
	Tyr228	1.20 x 10 ⁻³	0.146	1.12	-0.300	
	Tyr55	9.08 x 10 ⁻⁴	-0.119	1.81	-0.232	
	Trp185	9.71 x 10 ⁻⁶	-0.104	1.76	-0.178	
B (10)	Tyr314	1.38 x 10 ⁻²	-0.479	1.80	-0.236	
	Tyr224	5.96 x 10 ⁻³	-0.021	1.11	-0.312	
	Tyr55	1.54 x 10 ⁻³	-0.161	1.78	-0.250	
	Tyr228	1.25 x 10 ⁻³	0.056	1.13	-0.297	
	Tyr279	6.08 x 10 ⁻⁵	-0.076	1.85	-0.206	
A (30)	Tyr314	1.63 x 10 ⁻²	-0.293	1.81	-0.231	
	Tyr228	5.86 x 10 ⁻³	0.130	1.14	-0.290	

	Tyr224	3.39×10^{-3}	0.108	1.16	-0.272	.
	Tyr55	2.43×10^{-4}	-0.207	1.92	-0.168	
	Trp52	2.15×10^{-4}	-0.113	1.76	-0.178	
B (30)	Tyr224	1.68×10^{-2}	-0.038	1.08	-0.340	
	Tyr314	6.51×10^{-3}	-0.422	1.80	-0.234	
	Trp185	1.43×10^{-3}	-0.465	1.69	-0.216	
	Tyr55	9.70×10^{-4}	-0.210	1.80	-0.234	
	Tyr228	8.30×10^{-4}	0.097	1.12	-0.302	

a Data were taken from Ref 60.

b Net ES energy.

c Solvent reorganization energy

d ES energy between Iso anion and a donor cation